J. Fluid Mech. (2024), *vol.* 998, A24, doi:10.1017/jfm.2024.899

JFM PAPERS

Scaling laws for Rayleigh–Bénard convection between Navier-slip boundaries

F. Bleitner[1] **and C. Nobili**[2,†]

[1]Department of Mathematics, University of Hamburg, 20146 Hamburg, Germany

[2]School of Mathematics and Physics, University of Surrey, Guildford, Surrey GU2 7XH, UK

(Received 25 April 2024; revised 16 August 2024; accepted 11 September 2024)

We consider the two-dimensional Rayleigh–Bénard convection problem between Navier-slip fixed-temperature boundary conditions, and present a new upper bound for the Nusselt number (Nu). The result, based on a localization principle for the Nusselt number and an interpolation bound, exploits the regularity of the flow. On one hand our method yields a shorter proof of the celebrated result of Whitehead & Doering (*Phys. Rev. Lett.*, vol. 106, 2011, 244501) in the case of free-slip boundary conditions. On the other hand, its combination with a new, refined estimate for the pressure gives a substantial improvement of the interpolation bounds in Drivas *et al.* (*Phil. Trans. R. Soc.* A, vol. 380, issue 2225, 2022, 20210025) for slippery boundaries. A rich description of the scaling behaviour arises from our result: depending on the magnitude of the Prandtl number (Pr) and slip length, our upper bounds indicate five possible scaling laws (where Ra is the Rayleigh number): $Nu \sim (L_s^{-1}\,Ra)^{1/3}$, $Nu \sim (L_s^{-2/5}\,Ra)^{5/13}$, $Nu \sim Ra^{5/12}$, $Nu \sim Pr^{-1/6}(L_s^{-4/3}\,Ra)^{1/2}$ and $Nu \sim Pr^{-1/6}(L_s^{-1/3}\,Ra)^{1/2}$.

Key words: Navier–Stokes equations, turbulent convection

1. Introduction

In this paper, we consider a layer of fluid trapped between two parallel horizontal plates held at different temperatures. The dimensionless equations of motions for the Boussinesq approximation are

$$\frac{1}{Pr}\left(\partial_t \boldsymbol{u} + \boldsymbol{u}\cdot\nabla\boldsymbol{u}\right) - \Delta\boldsymbol{u} + \nabla p = Ra\,T\,\boldsymbol{e}_2, \tag{1.1}$$

$$\nabla\cdot\boldsymbol{u} = 0, \tag{1.2}$$

† Email address for correspondence: c.nobili@surrey.ac.uk

$$\partial_t T + \boldsymbol{u} \cdot \nabla T - \Delta T = 0, \tag{1.3}$$

where the Rayleigh number Ra is defined as

$$Ra = \frac{g\alpha\, \delta T\, h^3}{\kappa \nu}, \tag{1.4}$$

and the Prandtl number Pr is

$$Pr = \frac{\nu}{\kappa}. \tag{1.5}$$

In these definitions, g is the gravitational constant, α is the thermal expansion coefficient, ν is the kinematic viscosity, κ is the thermal diffusivity, h is the distance between the plates, and $\delta T = T_{bottom} - T_{top}$ is the temperature gap.

Lengths are measured in units of h, time in units of h^2/κ, and temperature in units of δT. In the rectangular domain $\Omega = [0, \Gamma] \times [0, 1]$ the velocity $\boldsymbol{u} = u_1(\boldsymbol{x}, t)\, \boldsymbol{e}_1 + u_2(\boldsymbol{x}, t)\, \boldsymbol{e}_2$ and temperature $T = T(\boldsymbol{x}, t)$ are initialized at $t = 0$, where

$$\boldsymbol{u}(\boldsymbol{x}, 0) = \boldsymbol{u}_0(\boldsymbol{x}), \tag{1.6}$$

$$T(\boldsymbol{x}, 0) = T_0(\boldsymbol{x}). \tag{1.7}$$

The boundary conditions for the temperature are

$$T = 0 \quad \text{at } x_2 = 1, \tag{1.8a}$$

$$T = 1 \quad \text{at } x_2 = 0, \tag{1.8b}$$

while we assume Navier-slip boundary conditions for the velocity field, i.e.

$$u_2 = 0,\ \partial_2 u_1 = -\frac{1}{L_s} u_1 \quad \text{at } x_2 = 1, \tag{1.9a}$$

$$u_2 = 0,\ \partial_2 u_1 = \frac{1}{L_s} u_1 \quad \text{at } x_2 = 0, \tag{1.9b}$$

where L_s is the constant slip length. Here, $x_2 = \boldsymbol{x} \cdot \boldsymbol{e}_2$. In the horizontal variable $x_1 = \boldsymbol{x} \cdot \boldsymbol{e}_1$, all variables, including the pressure $p = p(\boldsymbol{x}, t)$, are periodic.

We are interested in quantifying the heat transport in the upward direction as measured by the non-dimensional Nusselt number

$$Nu = \left\langle \int_0^1 (u_2 T - \partial_2 T)\, \mathrm{d}x_2 \right\rangle, \tag{1.10}$$

where

$$\langle \cdot \rangle = \limsup_{t \to \infty} \frac{1}{t} \int_0^t \frac{1}{\Gamma} \int_0^\Gamma (\cdot)\, \mathrm{d}x_1\, \mathrm{d}s. \tag{1.11}$$

This number, of utmost relevance in geophysics and industrial applications (Plumley & Julien 2019), is predicted to obey a power-law scaling of the type

$$Nu \sim Ra^{\alpha}\, Pr^{\beta}. \tag{1.12}$$

Although physical arguments suggest certain scaling exponents α and β (Malkus 1954; Kraichnan 1962; Spiegel 1971; Siggia 1994), where transitions between scalings could occur (Ahlers, Grossmann & Lohse 2009), these theories need to be validated. While experiments are expensive and difficult (Ahlers 2006), numerical studies are limited by the lack of computational power in reaching high-Rayleigh-number regimes (Plumley & Julien 2019). Even in two spatial dimensions, there have been recent debates about the presence/absence of evidence of the 'ultimate scaling' (scaling that holds in the regime of very large Rayleigh numbers) for the Nusselt number (Zhu *et al.* 2018, 2019; Doering, Toppaladoddi & Wettlaufer 2019; Doering 2020). We use mathematical analysis in order to derive universal upper bounds for the Nusselt number, which serve as a rigorous indication for the scaling exponents holding in the turbulent regime $Ra \to \infty$. The properties of boundary layers and their thicknesses play a central role in the scaling laws for the Nusselt number in Rayleigh–Bénard convection (see Nobili (2023) and references therein). For this reason, it is interesting to study how heat transport properties change when varying the boundary conditions. In particular, we ask the following question: are there boundary conditions inhibiting or enhancing heat transport compared to the classical no-slip boundary conditions? While many theoretical studies focus on no-slip boundary conditions (Doering & Constantin 1996, 2001; Doering, Otto & Reznikoff 2006; Otto & Seis 2011; Goluskin & Doering 2016; Tobasco & Doering 2017), other reasonable boundary conditions have been far less explored. In the early 2000s, Ierley, Kerswell & Plasting (2006) considered the Rayleigh–Bénard convection problem at infinite Prandtl number and free-slip boundary conditions; their computational result $Nu \lesssim Ra^{5/12}$ is obtained by combining the Busse asymptotic expansion in multiple boundary layer solutions (multi-α solutions) and the Constantin and Doering background field method approach (Doering & Constantin 1994, 1996). Inspired by this result and a numerical study in the thesis of Otero (2002), Doering and Whitehead rigorously proved

$$Nu \lesssim Ra^{5/12} \tag{1.13}$$

for the two-dimensional finite Prandtl model (Whitehead & Doering 2011) and for the three-dimensional infinite Prandtl number model (Whitehead & Doering 2012) using an elaborate application of the background field method. By a perturbation argument around Stokes equations, Wang & Whitehead (2013) proved

$$Nu \lesssim Ra^{5/12} + Gr^2\, Ra^{1/4} \tag{1.14}$$

in three dimensions for small Grashof number ($Gr = Ra/Pr$).

In many physical situations, the Navier-slip boundary conditions are used to describe the presence of slip at the solid–liquid interface (Neto *et al.* 2005; Uthe, Sader & Pelton 2022). We notice that for any finite $L_s > 0$, these conditions imply vorticity production at the boundary. In the limit of infinite slip length, the Navier-slip boundary conditions reduce to free-slip boundary conditions, while in the limit $L_s \to 0$, they converge to the no-slip boundary conditions.

Inspired by the seminal paper of Whitehead & Doering (2011), Drivas, Nguyen and the second author of this paper considered the two-dimensional Rayleigh–Bénard convection model with Navier-slip boundary conditions, and rigorously proved the upper bound

$$Nu \lesssim Ra^{5/12} + L_s^{-2}\, Ra^{1/2} \tag{1.15}$$

when $Pr \geq Ra^{3/4} L_s^{-1}$ and $L_s \gtrsim 1$ (Drivas, Nguyen & Nobili 2022). The authors refer to (1.15) as an interpolation bound: assuming $L_s \sim Ra^{\alpha}$ with $\alpha \geq 0$ (the justification of this choice can be found in the appendix of Bleitner & Nobili 2024), it can be deduced easily that

$$Nu \lesssim \begin{cases} Ra^{5/12}, & \text{if } \alpha \geq \frac{1}{24}, \\ Ra^{1/2-2\alpha}, & \text{if } 0 \leq \alpha \leq \frac{1}{24}. \end{cases} \tag{1.16}$$

In Bleitner & Nobili (2024), the authors generalized the result in Drivas *et al.* (2022) to the case of rough walls and Navier-slip boundary conditions, proving interpolation bounds exhibiting explicit dependency on the spatially varying friction coefficient and curvature.

Given the model (1.1), (1.2), (1.3) with (1.8) and (1.9), the objective of this paper is twofold: on one hand we want to apply the so-called direct method (as outlined in Otto & Seis 2011) to derive upper bounds on the Nusselt number exhibiting a transparent relation with the thermal boundary layer's thickness. For discussions about different approaches to derive bounds on the Nusselt number, we refer the reader to Chernyshenko (2022) and references therein. On the other hand, we aim to improve the bound in Drivas *et al.* (2022) by refining the estimates on the pressure. Our new result is stated in the following theorem.

THEOREM 1.1. *Suppose* $\boldsymbol{u}_0 \in W^{1,4}$ *and* $0 \leq T_0 \leq 1$.

If $L_s = \infty$ *(i.e.* $\boldsymbol{u}$ *satisfies free-slip boundary conditions), then*

$$Nu \lesssim Ra^{5/12}. \tag{1.17}$$

If $1 \leq L_s < \infty$, *then*

$$Nu \lesssim Ra^{5/12} + L_s^{-1/6}\, Pr^{-1/6}\, Ra^{1/2}. \tag{1.18}$$

If $0 < L_s < 1$, *then*

$$Nu \lesssim L_s^{-1/3}\, Ra^{1/3} + L_s^{-2/3}\, Pr^{-1/6}\, Ra^{1/2} + L_s^{-2/13}\, Ra^{5/13} + Ra^{5/12}. \tag{1.19}$$

We reserve the discussion on physical implications of this result for the conclusions, in § 4. We first remark that for $L_s \geq 1$, this result improves the upper bound in (1.15): in fact, if $L_s \sim Ra^{\alpha}$, with $\alpha \geq 0$, then our new result yields

$$Nu \lesssim \begin{cases} Ra^{5/12}, & \text{if } Pr \geq Ra^{1/2-\alpha}, \\ Pr^{-1/6}\, Ra^{1/2-\alpha/6}, & \text{if } Pr \leq Ra^{1/2-\alpha}. \end{cases} \tag{1.20}$$

In particular, when $\alpha = 0$, we notice a crossover at $Pr \sim Ra^{1/2}$ between the $Ra^{1/2}$ and $Pr^{-1/6}\, Ra^{1/2}$ scaling regimes. This is reminiscent of the upper bound in Choffrut, Nobili & Otto (2016) for no-slip boundary conditions. Our result also covers the case $0 < L_s < 1$, and in this region, we can detect four scaling regimes depending on the magnitude of the Prandtl number and $L_s < 1$. The dominating terms in (1.18) and (1.19) are summarized in table 1. Observe that for $Pr \to \infty$, the term $L_s^{-1/3}\, Ra^{1/3}$ is dominating in the region $0 < L_s < Ra^{-2/7}$. On one hand, when $Pr \to \infty$, this seems to indicate the (expected) transition from Navier-slip to no-slip boundary conditions in the bounds. In order to contextualize this remark, we recall that for no-slip boundary conditions ($L_s = 0$), the upper bound $Nu \lesssim Ra^{1/3}$ was proven when $Pr = \infty$ (Otto & Seis 2011) and when $Pr \gtrsim Ra^{1/3}$ (Choffrut *et al.* 2016). On the other hand, we stress that our bounding method breaks down in the limit $L_s \to 0$, and consequently all but the last scaling prefactors in (1.19) blow up.

Differently from the result in Whitehead & Doering (2011), the proof of our theorem does not rely on the background field method but rather exploits the regularity properties

	Assumptions	Bound
$Ra^{11/7} \le Pr$	$Ra^{-5/24} \le L_s$	$Nu \lesssim Ra^{5/12}$
	$Ra^{-2/7} \le L_s \le Ra^{-5/24}$	$Nu \lesssim L_s^{-2/13}\, Ra^{5/13}$
	$Pr^{-1/2}\, Ra^{1/2} \le L_s \le Ra^{-2/7}$	$Nu \lesssim L_s^{-1/3}\, Ra^{1/3}$
	$L_s \le Pr^{-1/2}\, Ra^{1/2}$	$Nu \lesssim L_s^{-2/3}\, Pr^{-1/6}\, Ra^{1/2}$
$Ra^{4/3} \le Pr \le Ra^{11/7}$	$Ra^{-5/24} \le L_s$	$Nu \lesssim Ra^{5/12}$
	$Pr^{-13/40}\, Ra^{9/40} \le L_s \le Ra^{-5/24}$	$Nu \lesssim L_s^{-2/13}\, Ra^{5/13}$
	$L_s \le Pr^{-13/40}\, Ra^{9/40}$	$Nu \lesssim L_s^{-2/3}\, Pr^{-1/6}\, Ra^{1/2}$
$Ra^{1/2} \le Pr \le Ra^{4/3}$	$Pr^{-1/4} Ra^{1/8} \le L_s$	$Nu \lesssim Ra^{5/12}$
	$L_s \le Pr^{-1/4}\, Ra^{1/8}$	$Nu \lesssim L_s^{-2/3}\, Pr^{-1/6}\, Ra^{1/2}$
$Pr \le Ra^{1/2}$	$Pr^{-1}\, Ra^{1/2} \le L_s$	$Nu \lesssim Ra^{5/12}$
	$1 \le L_s \le Pr^{-1}\, Ra^{1/2}$	$Nu \lesssim L_s^{-1/6}\, Pr^{-1/6}\, Ra^{1/2}$
	$L_s \le 1$	$Nu \lesssim L_s^{-2/3}\, Pr^{-1/6}\, Ra^{1/2}$

Table 1. Overview of the results in Theorem 1.1. The colouring corresponds to the cases $L_s \le 1$ and $1 \le L_s$. In all the other (uncoloured) cases, L_s may be smaller or larger than 1.

of the flow through a localization principle. In fact, the Nusselt number can be localized in the vertical variable:

$$Nu = \frac{1}{\delta}\left\langle \int_0^\delta (u_2 T - \partial_2 T)\,\mathrm{d}x_2 \right\rangle \le \frac{1}{\delta}\left\langle \int_0^\delta u_2 T\,\mathrm{d}x_2 \right\rangle + \frac{1}{\delta}. \tag{1.21}$$

Here, we used the boundary conditions for the temperature and the maximum principle $\sup_x |T(x, t)| \le 1$ for all t. Notice that this localization principle comes from the fact that the (long-time and horizontal average of the) heat flux is the same for each $x_2 \in (0, 1)$, and this can be deduced by merely using the non-penetration boundary conditions $u_2 = 0$ at $x_2 = 0$, $x_2 = 1$ (see the proof of Lemma 2.1 below).

The second crucial point in our proof is the interpolation inequality

$$\frac{1}{\delta}\left\langle \int_0^\delta u_2 T\,\mathrm{d}x_2 \right\rangle \le \frac{1}{2}\left\langle \int_0^1 |\partial_2 T|^2\,\mathrm{d}x_2 \right\rangle + C\delta^3 \left\langle \int_0^1 |\omega|^2\,\mathrm{d}x_2 \right\rangle^{1/2} \left\langle \int_0^1 |\partial_1 \omega|^2\,\mathrm{d}x_2 \right\rangle^{1/2}, \tag{1.22}$$

where C is some positive constant, which was first derived (in a slightly different form) in Drivas *et al.* (2022); it is proved in Lemma 3.1 below. We again observe that this bound holds only relying on the assumption $u_2 = 0$ at the boundaries $x_2 = 0$, $x_2 = 1$.

In Lemma 2.5, we prove the new pressure estimate

$$\|p\|_{H^1} \le C\left(\frac{1}{L_s}\,\|\partial_2 \boldsymbol{u}\|_{L^2} + \frac{1}{Pr}\,\|\omega\|_{L^2}\,\|\omega\|_{L^r} + Ra\,\|T\|_{L^2}\right), \tag{1.23}$$

where L^2 is the space of square integrable functions, while H^1 is the space of functions in L^2 with square integrable gradients. The space L^r instead consists of functions whose rth power is integrable. See definitions in (1.25). Notice that the improvement (compared to the pressure estimate in Proposition 2.7 in Drivas *et al.* 2022) lies in the first term on the right-hand side, stemming from the new trace-type estimate

$$\left| \int_0^{\Gamma} (p\, \partial_1 u_1|_{x_2=1} + p\, \partial_1 u_1|_{x_2=0})\, \mathrm{d}x_1 \right| \leq 3\, \|p\|_{H^1}\, \|\partial_2 \boldsymbol{u}\|_{L^2}, \tag{1.24}$$

used to control the boundary terms in the H^1 pressure identity (2.49). We observe that the new pressure estimate enables us to treat the case of small slip length, i.e. $0 < L_s \leq 1$. This small slip length regime was not treatable in Drivas *et al.* (2022); see Remark 2.6.

1.1. *Organization and notations*

The paper is divided in two sections: in § 2, we prove all the *a priori* estimates that we will need in order to prove the main theorem in § 3. The crucial localization and interpolation lemmas are proven in Lemmas 2.1 and 3.1, respectively. The improvement of the upper bounds on the Nusselt number stems from the new pressure estimates in Lemma 2.5. In § 4, we contextualize our result and give a physical interpretation of our bounds.

Throughout the paper, we will use the following Lebesgue and Sobolev norms:

$$\|f\|_{L^p}^p = \int_{\Omega} |f|^p \, \mathrm{d}x, \quad \|f\|_{W^{1,p}}^p = \int_{\Omega} |f|^p \, \mathrm{d}x + \int_{\Omega} |\nabla f|^p \, \mathrm{d}x, \quad \|f\|_{H^1} = \|f\|_{W^{1,2}}, \tag{1.25}$$

for any $1 \leq p < \infty$.

2. Identities and *a priori* bounds

In this section, we derive *a priori* bounds for the Rayleigh–Bénard convection problem with Navier-slip boundary conditions. These will be used in the proof of Theorem 1.1 in § 3.

Recall that the temperature equation enjoys a maximum principle: if $0 \leq T_0(\boldsymbol{x}) \leq 1$, then

$$0 \leq T(\boldsymbol{x}, t) \leq 1, \quad \text{for all } \boldsymbol{x}, t. \tag{2.1}$$

The following lemma will allow us to localize the Nusselt number in a strip of height $\delta > 0$, indicating the thermal boundary layer. This is the key ingredient of the direct method, and will be used later to bound the heat transfer.

LEMMA 2.1 (Localization of the Nusselt number). *The Nusselt number Nu defined in (1.10) is independent of x_2, i.e.*

$$Nu = \langle u_2 T - \partial_2 T \rangle, \quad \textit{for all } x_2 \in [0, 1]. \tag{2.2}$$

In particular, for any $\delta \in (0, 1)$, we have

$$Nu = \frac{1}{\delta} \left\langle \int_0^{\delta} (u_2 T - \partial_2 T)\, \mathrm{d}x_2 \right\rangle. \tag{2.3}$$

Proof. Taking the long-time and horizontal average of the equation for T, we have

$$0 = \langle \partial_t T \rangle + \langle \nabla \cdot (\boldsymbol{u} T - \nabla T) \rangle = \partial_2 \langle u_2 T - \partial_2 T \rangle. \tag{2.4}$$

Hence $\langle u_2 T - \partial_2 T \rangle$ is constant in x_2, proving (2.2). The identity (2.3) is a direct consequence of (2.2).

Notice that from the boundary condition for T at $x_2 = 0$, i.e. (1.8*b*), and the maximum principle (2.1), it follows that

$$-\int_0^\delta \partial_2 T \,\mathrm{d}x_2 = -T(x_1, \delta) + 1 \le 1. \tag{2.5}$$

As a consequence, we obtain

$$Nu \le \frac{1}{\delta}\left\langle \int_0^\delta u_2 T \,\mathrm{d}x_2 \right\rangle + \frac{1}{\delta}. \tag{2.6}$$

Thanks to (2.2), we can now derive another useful identity relating temperature gradients (naturally emerging in (2.46) and (3.1)) to the Nusselt number.

LEMMA 2.2 (Representation of the Nusselt number). *The Nusselt number, defined in (1.10), has the following alternative representation:*

$$Nu = \left\langle \int_0^1 |\nabla T|^2 \,\mathrm{d}x_2 \right\rangle. \tag{2.7}$$

Proof. Testing (1.3), the temperature equation with T, and integrating by parts, we obtain

$$\frac{1}{2}\frac{\mathrm{d}}{\mathrm{d}t}\|T\|_{L^2}^2 = -\|\nabla T\|_{L^2}^2 - \int_0^\Gamma \partial_2 T|_{x_2=0} \,\mathrm{d}x_1, \tag{2.8}$$

where we used the incompressibility condition (1.2), the non-penetration condition $\boldsymbol{u}\cdot\boldsymbol{e}_2 = u_2 = 0$ at $x_2 = \{0, 1\}$, and the boundary conditions (1.8) for T. The statement follows from taking the long-time averages, observing that $\limsup_{t\to\infty}\int_0^t (\mathrm{d}/\mathrm{d}s)(1/\Gamma)\int_0^\Gamma\int_0^1 |T|^2 \,\mathrm{d}x_2\,\mathrm{d}x_1\,\mathrm{d}s = 0$ thanks to the maximum principle for T (2.1), and using $Nu = \langle u_2 T - \partial_2 T\rangle|_{x_2=0}$ by (2.2).

The subsequent Lemma 2.3 provides a bound on the long-time (and spatial) average of the velocity gradient, naturally arising from the interpolation estimate in Lemma 3.1. Moreover this bound will be used to control the vorticity gradient in Lemma 2.4.

LEMMA 2.3 (Energy). *Let* $0 < L_s < \infty$, *and suppose that* $\boldsymbol{u}_0 \in L^2$. *Then there exists a constant* $C = C(\Gamma) > 0$ *such that*

$$\|\boldsymbol{u}(t)\|_{L^2} \le \|\boldsymbol{u}_0\|_{L^2} + C\max\{1, L_s\}\,Ra \tag{2.9}$$

for all times $t \in [0, \infty)$, *and*

$$\left\langle \int_0^1 |\nabla \boldsymbol{u}|^2 \,\mathrm{d}x_2 \right\rangle \le Nu\,Ra. \tag{2.10}$$

If $L_s = \infty$, *then the bound* (2.9) *simplifies to*

$$\|\boldsymbol{u}(t)\|_{L^2} \le \|\boldsymbol{u}_0\|_{L^2} + C\,Ra, \tag{2.11}$$

and (2.10) *remains valid.*

https://doi.org/10.1017/jfm.2024.899 Published online by Cambridge University Press

Proof. At first, we assume $0 < L_s < \infty$ and test the velocity equation (1.1) with $\boldsymbol{u}$, integrate by parts, and use the boundary conditions (1.9) for u and the incompressibility condition (1.2) to find

$$\frac{1}{2\,Pr}\frac{\mathrm{d}}{\mathrm{d}t}\int_\Omega |\boldsymbol{u}|^2\,\mathrm{d}x + \int_\Omega |\nabla \boldsymbol{u}|^2\,\mathrm{d}x + \frac{1}{L_s}\int_0^\Gamma (u_1^2|_{x_2=0} + u_1^2|_{x_2=1})\,\mathrm{d}x_1 = Ra\int_\Omega Tu_2\,\mathrm{d}x. \tag{2.12}$$

The fundamental theorem of calculus implies

$$u_1(\boldsymbol{x}) = u_1(x_1, 0) + \int_0^{x_2} \partial_2 u_1(x_1, z)\,\mathrm{d}z, \tag{2.13}$$

and using Young's and Hölder's inequality gives

$$u_1^2(\boldsymbol{x}) = u_1^2(x_1, 0) + 2u_1(x_1, 0)\int_0^{x_2} \partial_2 u_1(x_1, z)\,\mathrm{d}z + \left(\int_0^{x_2} \partial_2 u_1(x_1, z)\,\mathrm{d}z\right)^2 \tag{2.14}$$

$$\leq 2u_1^2(x_1, 0) + 2\left(\int_0^{x_2} |\partial_2 u_1(x_1, z)|\,\mathrm{d}z\right)^2 \tag{2.15}$$

$$\leq 2u_1^2(x_1, 0) + 2\int_0^{x_2} |\partial_2 u_1(x_1, z)|^2\,\mathrm{d}z, \tag{2.16}$$

which after integration implies

$$\|u_1\|_{L^2}^2 \leq 2\int_0^\Gamma u_1^2|_{x_2=0}\,\mathrm{d}x_1 + 2\|\partial_2 u_1\|_{L^2}^2. \tag{2.17}$$

By (1.9), one has $u_2 = 0$ on the boundaries, therefore the analogous estimate shows that

$$\|u_2\|_{L^2}^2 \leq \|\partial_2 u_2\|_{L^2}^2. \tag{2.18}$$

The full vector norm of the velocity can now be split into the norms of its components, and by (2.17) and (2.18), we have

$$\|\boldsymbol{u}\|_{L^2}^2 = \|u_1\|_{L^2}^2 + \|u_2\|_{L^2}^2 \tag{2.19}$$

$$\leq 2\left(\|\partial_2 u_1\|_{L^2}^2 + \int_0^\Gamma (u_1^2|_{x_2=0} + u_1^2|_{x_2=1})\,\mathrm{d}x_1 + \|\partial_2 u_2\|_{L^2}^2\right) \tag{2.20}$$

$$\leq 2\left(\|\nabla \boldsymbol{u}\|_{L^2}^2 + \int_0^\Gamma (u_1^2|_{x_2=0} + u_1^2|_{x_2=1})\,\mathrm{d}x_1\right), \tag{2.21}$$

which applied to (2.12) yields

$$\begin{aligned}\frac{1}{2\,Pr}\frac{\mathrm{d}}{\mathrm{d}t}\int_\Omega |\boldsymbol{u}|^2\,\mathrm{d}x &+ \frac{1}{C}\min\{1, L_s^{-1}\}\,\|\boldsymbol{u}\|_{L^2}^2\\ &\leq Ra\int_\Omega Tu_2\,\mathrm{d}x \leq Ra\,\|T\|_{L^2}\,\|u_2\|_{L^2}\\ &\leq \frac{1}{4\epsilon}\,\|T\|_{L^2}^2\,Ra^2 + \epsilon\,\|u_2\|_{L^2}^2 \leq \frac{1}{4\epsilon}\,\Gamma\,Ra^2 + \epsilon\,\|u_2\|_{L^2}^2,\end{aligned} \tag{2.22}$$

for some constant $C > 0$, where we used Hölder's inequality, Young's inequality and $\|T\|_{L^\infty} \leq 1$ because of the maximum principle (2.1). Setting $\epsilon = (1/2C)\min\{1, L_s^{-1}\}$ implies

$$\frac{1}{Pr}\frac{\mathrm{d}}{\mathrm{d}t}\|\boldsymbol{u}\|_{L^2}^2 + \frac{1}{C}\min\{1, L_s^{-1}\}\,\|\boldsymbol{u}\|_{L^2}^2 \leq C\max\{1, L_s\}\,\Gamma\, Ra^2, \tag{2.23}$$

and Grönwall's inequality now yields (2.9). Taking the long-time average of (2.12), using (2.9), one has

$$\left\langle \int_0^1 |\nabla \boldsymbol{u}|^2\,\mathrm{d}x_2 \right\rangle + \frac{1}{L_s}\left\langle (u_1^2|_{x_2=0} + u_1^2|_{x_2=1}) \right\rangle = Ra\left\langle \int_0^1 Tu_2\,\mathrm{d}x_2 \right\rangle. \tag{2.24}$$

The claim follows by observing that, due to the boundary conditions for T, we have

$$Nu = \left\langle \int_0^1 Tu_2\,\mathrm{d}x_2 \right\rangle + 1. \tag{2.25}$$

If $L_s = \infty$, then integrating the first component of (1.1) in space yields

$$\frac{1}{Pr}\frac{\mathrm{d}}{\mathrm{d}t}\int_\Omega u_1\,\mathrm{d}x = -\frac{1}{Pr}\int_\Omega \boldsymbol{u}\cdot\nabla u_1\,\mathrm{d}x + \int_\Omega \Delta u_1\,\mathrm{d}x - \int_\Omega \partial_1 p. \tag{2.26}$$

The first term on the right-hand side of (2.26) vanishes after integration by parts due to the incompressibility condition (1.2) and the boundary conditions (1.9). Similarly, the second and third terms on the right-hand side vanish due to Stokes' theorem, (1.9) and the periodicity in the horizontal direction, showing that the spatial average of u_1 is conserved. Therefore, due to the Galilean symmetry of the system, we can assume u_1 to be average free. Consequently, the Poincaré inequality (Evans 1998, § 5.8.1) implies that there exists a constant $C = C(\Gamma) > 0$ such that

$$\|u_1\|_{L^2} \leq C\,\|\nabla u_1\|_{L^2}, \tag{2.27}$$

and combined with (2.18), we find

$$\|\boldsymbol{u}\|_{L^2} \leq C\,\|\nabla \boldsymbol{u}\|_{L^2}, \tag{2.28}$$

the analogue of (2.21). Using (2.28) instead of (2.21), the arguments corresponding to (2.22)–(2.25) yield the bounds for $L_s = \infty$.

In order to bound the second derivatives of $\boldsymbol{u}$, we will exploit the equation for the vorticity $\omega = \partial_1 u_2 - \partial_2 u_1$:

$$Pr^{-1}\,(\partial_t\omega + \boldsymbol{u}\cdot\nabla\omega) - \Delta\omega = Ra\,\partial_1 T \quad \text{in } \Omega, \tag{2.29}$$

$$\omega = \frac{1}{L_s}u_1 \quad \text{at } x_2 = 1, \tag{2.30}$$

$$\omega = -\frac{1}{L_s}u_1 \quad \text{at } x_2 = 0. \tag{2.31}$$

Note that in the two-dimensional setting, the vorticity is a scalar function, and for any $0 < L_s \leq \infty$, we have

$$\|\nabla\boldsymbol{u}\|_{L^2} = \|\omega\|_{L^2}, \quad \|\nabla\boldsymbol{u}\|_{L^p} \leq C\,\|\omega\|_{L^p}. \tag{2.32}$$

While the identity in L^2 follows from a direct computation, the inequality in L^p follows by elliptic regularity; in fact, let ψ be the the stream function for $\boldsymbol{u}$, i.e. $\boldsymbol{u} = \nabla^\perp \psi = (-\partial_2 \psi, \partial_1 \psi)$. Since $\partial_1 \psi = u_2 = 0$ at $x_2 = 1$ and $x_2 = 0$, and ψ is defined only up to a constant, we can choose it such that $\psi = 0$ on $x_2 = 0$. Therefore, using the fundamental theorem of calculus,

$$\psi(x_1, 1) = \psi(x_1, 0) + \int_0^1 \partial_2 \psi(x_1, z)\,\mathrm{d}z = -\int_0^1 u_1(x_1, z)\,\mathrm{d}z, \tag{2.33}$$

and since ψ is constant at $x_2 = 1$, averaging (2.33) in x_1 yields $\psi(x_1, 1) = -(1/\Gamma)\int_\Omega u_1\,\mathrm{d}x$. Combining these observations with the direct computation $\Delta\psi = \nabla^\perp \cdot \nabla^\perp \psi = \nabla^\perp \cdot \boldsymbol{u} = \omega$ shows that ψ is a solution of

$$\Delta\psi = \omega \quad \text{in } \Omega, \tag{2.34}$$

$$\psi = -\frac{1}{\Gamma}\int_\Omega u_1\,\mathrm{d}x \quad \text{at } x_2 = 1, \tag{2.35}$$

$$\psi = 0 \quad \text{at } x_2 = 0, \tag{2.36}$$

and $\tilde{\psi} = \psi + x_2 \int_\Omega u_1\,\mathrm{d}\boldsymbol{x}$ solves

$$\Delta\tilde{\psi} = \omega \quad \text{in } \Omega, \tag{2.37}$$

$$\psi = 0 \quad \text{at } x_2 \in \{0, 1\}. \tag{2.38}$$

One has

$$\|\nabla \boldsymbol{u}\|_{L^p}^p = \|\nabla u_1\|_{L^p}^p + \|\nabla u_2\|_{L^p}^p = \|-\nabla\partial_2\psi\|_{L^p}^p + \|\nabla\partial_1\psi\|_{L^p}^p \tag{2.39}$$

$$\leq \|\nabla^2\psi\|_{L^p}^p + \|\nabla^2\psi\|_{L^p}^p = \|\nabla^2\tilde{\psi}\|_{L^p}^p + \|\nabla^2\tilde{\psi}\|_{L^p}^p \leq C\|\omega\|_{L^p}^p, \tag{2.40}$$

where we used the Calderon–Zygmund estimate (Gilbarg & Trudinger 1977, § 9.4) in the last inequality.

The following lemma provides a higher-order version of Lemma 2.3. The uniform in time bound will later be used to control the pressure terms arising due to the vorticity production on the boundary, while the long-time average estimate will be used in the proof of the main theorem to estimate the thickness of the thermal boundary layer.

LEMMA 2.4 (Enstrophy). *Suppose $\boldsymbol{u}_0 \in W^{1,4}$ and $0 < L_s \leq \infty$. Then there exists a constant $C = C(\Gamma) > 0$ such that for all $t > 0$,*

$$\|\omega(t)\|_{L^4} \leq C \max\left\{1, L_s^{-3}\right\}(\|\boldsymbol{u}_0\|_{W^{1,4}} + Ra) \tag{2.41}$$

and

$$\left\langle \int_0^1 |\nabla\omega|^2\,\mathrm{d}x_2 \right\rangle \leq \frac{1}{L_s}\left|\langle p\,\partial_1 u_1|_{x_2=1}\rangle + \langle p\,\partial_1 u_1|_{x_2=0}\rangle\right| + Nu\,Ra^{3/2}. \tag{2.42}$$

Proof. For the proof of (2.41), we refer the reader to Drivas *et al.* (2022, Lemma 2.11), where the case $L_s \geq 1$ is covered. The same argument also yields the bound in the case $L_s < 1$. Testing the equation with ω and integrating by parts, we obtain

$$\frac{1}{2\,Pr}\frac{\mathrm{d}}{\mathrm{d}t}\left(\|\omega\|_{L^2}^2 + \frac{1}{L_s}\|u_1\|_{L^2(x_2=0)}^2 + \frac{1}{L_s}\|u_1\|_{L^2(x_2=1)}^2\right) + \|\nabla\omega\|_{L^2}^2\,\mathrm{d}x \\ + \frac{1}{L_s}\left[\int_0^{\Gamma}\partial_1 u_1 p|_{x_2=0}\,\mathrm{d}x_1 + \int_0^{\Gamma}\partial_1 u_1 p|_{x_2=1}\mathrm{d}x_1\right] = Ra\int_{\Omega}\omega\,\partial_1 T\,\mathrm{d}x, \tag{2.43}$$

where we used $-\partial_2\omega = \Delta u_1 = (1/Pr)(\partial_t u_1 + (\boldsymbol{u}\cdot\nabla)u_1) - \partial_1 p$ and the fact that $\omega(\boldsymbol{u}\cdot\nabla)u_1 = \pm(1/L_s)u_1^2\,\partial_1 u_1$ at $x_2 = \{0, 1\}$ vanishes after integration (in x_1) due to periodicity. We integrate (2.43) in time, and notice that thanks to (2.32) and the trace estimate (Evans 1998, § 5.5), the first bracket on the left-hand side is bounded by the H^1-norm of $\boldsymbol{u}$:

$$\|\omega\|_{L^2}^2 + \frac{1}{L_s}\|u_1\|_{L^2(x_2=0)}^2 + \frac{1}{L_s}\|u_1\|_{L^2(x_2=1)}^2 \leq C(L_s)\,\|\boldsymbol{u}\|_{H^1}^2. \tag{2.44}$$

Note also that due to Hölder's inequality, (2.41) additionally yields

$$\|\omega(t)\|_{L^2} \leq C\max\left\{1, L_s^{-3}\right\}(\|\boldsymbol{u}_0\|_{W^{1,4}} + Ra), \tag{2.45}$$

which, combined with (2.9) and (2.32), implies that $\|\boldsymbol{u}(t)\|_{H^1}$ is universally bounded in time. Therefore, claim (2.42) follows from taking the space and long-time average of (2.43), using the fact that the long-time average of the first term in (2.43) vanishes due to the argument above, and observing

$$\left\langle\int_{\Omega}\omega\partial_1 T\,\mathrm{d}x_2\right\rangle \leq \left\langle\int_{\Omega}|\omega|^2\,\mathrm{d}x_2\right\rangle^{1/2}\left\langle\int_{\Omega}|\nabla T|^2\,\mathrm{d}x_2\right\rangle^{1/2} \leq (Nu\,Ra)^{1/2}\,Nu^{1/2}, \tag{2.46}$$

where we used (2.32), (2.10) and (2.7).

Notice that the pressure term appears at the boundary in (2.42), and for this reason, we need to control its H^1-norm. The next lemma will provide control for this term. Taking the divergence of (1.1), it is easy to see that the pressure p satisfies

$$\Delta p = -\frac{1}{Pr}\nabla\boldsymbol{u}^{\mathrm{T}} : \nabla\boldsymbol{u} + Ra\,\partial_2 T \quad \text{in } \Omega, \tag{2.47a}$$

$$\partial_2 p = \frac{1}{L_s}\partial_1 u_1 \quad \text{at } x_2 = 1, \tag{2.47b}$$

$$-\partial_2 p = \frac{1}{L_s}\partial_1 u_1 - Ra \quad \text{at } x_2 = 0, \tag{2.47c}$$

where the boundary conditions are derived by tracing the second component of (1.1) on the boundary.

LEMMA 2.5 (Pressure bound). *Let $r > 2$. Then there exists a constant $C = C(r, \Gamma) > 0$ such that*

$$\|p\|_{H^1} \leq C\left(\frac{1}{L_s}\|\partial_2\boldsymbol{u}\|_{L^2} + \frac{1}{Pr}\|\omega\|_{L^2}\|\omega\|_{L^r} + Ra\,\|T\|_{L^2}\right). \tag{2.48}$$

Proof. The proof is a consequence of the following two claims:

$$\|\nabla p\|_{L^2}^2 = \frac{1}{L_s}\int_0^{\Gamma} (p\,\partial_1 u_1|_{x_2=1} + p\,\partial_1 u_1|_{x_2=0})\,\mathrm{d}x_1 + \frac{1}{Pr}\int_{\Omega} p\,\nabla \boldsymbol{u}^{\mathrm{T}} : \nabla \boldsymbol{u}\,\mathrm{d}x + Ra\int_{\Omega} \partial_2 p T\,\mathrm{d}x, \tag{2.49}$$

$$\left|\int_0^{\Gamma} (p\,\partial_1 u_1|_{x_2=1} + p\,\partial_1 u_1|_{x_2=0})\,\mathrm{d}x_1\right| \leq 3\,\|p\|_{H^1}\,\|\partial_2 \boldsymbol{u}\|_{L^2}. \tag{2.50}$$

In fact, applying the Poincaré inequality (p can be assumed to have zero mean, since $p - \langle p\rangle$ satisfies (2.47)) and combining (2.49) and (2.50), we obtain

$$\|p\|_{H^1}^2 \lesssim \frac{1}{L_s}\int_0^{\Gamma} (p\,\partial_1 u_1|_{x_2=1} + p\,\partial_1 u_1|_{x_2=0})\,\mathrm{d}x_1 + \frac{1}{Pr}\int_{\Omega} p\,\nabla \boldsymbol{u}^{T} : \nabla \boldsymbol{u}\,\mathrm{d}x + Ra\int_{\Omega} \partial_2 p T\,\mathrm{d}x \tag{2.51}$$

$$\lesssim L_s^{-1}\,\|p\|_{H^1}\,\|\partial_2 \boldsymbol{u}\|_{L^2} + Pr^{-1}\,\|p\|_{L^q}\,\|\nabla \boldsymbol{u}\|_{L^2}\,\|\nabla \boldsymbol{u}\|_{L^r} + Ra\,\|p\|_{H^1}\,\|T\|_{L^2} \tag{2.52}$$

$$\lesssim L_s^{-1}\,\|p\|_{H^1}\,\|\partial_2 \boldsymbol{u}\|_{L^2} + Pr^{-1}\,\|p\|_{H^1}\,\|\nabla \boldsymbol{u}\|_{L^2}\,\|\nabla \boldsymbol{u}\|_{L^r} + Ra\,\|p\|_{H^1}\,\|T\|_{L^2}, \tag{2.53}$$

where $f \lesssim g$ indicates that there exists $C > 0$ such that $f \leq Cg$, and q and r are related by $1/p + 1/r = 1/2$. In (2.52) we used the trace estimate, and in (2.53) the fact that $\|p\|_{L^q} \leq C\,\|p\|_{H^1}$ for any $q \in (2, \infty)$ by Sobolev embedding in bounded domains. It is left to prove the claims.

Argument for (2.49). Integrating by parts and using (2.47*a*) gives

$$\|\nabla p\|_{L^2}^2 = \int_0^{\Gamma} p\,\partial_2 p|_{x_2=1}\,\mathrm{d}x_1 - \int_0^{\Gamma} p\,\partial_2 p|_{x_2=0}\,\mathrm{d}x_1 - \int_{\Omega} p\,\Delta p\,\mathrm{d}x \tag{2.54}$$

$$= \frac{1}{L_s}\int_0^{\Gamma} p(\partial_1 u_1|_{x_2=1} + \partial_1 u_1|_{x_2=0})\,\mathrm{d}x_1 - Ra\int_0^{\Gamma} p|_{x_2=0}\,\mathrm{d}x_1 + \frac{1}{Pr}\int_{\Omega} p\,\nabla \boldsymbol{u}^{\mathrm{T}} : \nabla \boldsymbol{u}\,\mathrm{d}x - Ra\int_{\Omega} \partial_2 T p\,\mathrm{d}x \tag{2.55}$$

$$= \frac{1}{L_s}\int_0^{\Gamma} p(\partial_1 u_1|_{x_2=1} + \partial_1 u_1|_{x_2=0})\,\mathrm{d}x_1 + \frac{1}{Pr}\int_{\Omega} p\,\nabla \boldsymbol{u}^{\mathrm{T}} : \nabla \boldsymbol{u}\,\mathrm{d}x + Ra\int_{\Omega} T\,\partial_2 p\,\mathrm{d}x, \tag{2.56}$$

where in the last identity we used $-Ra\int_{\Omega} \partial_2 T p - Ra\int_0^{\Gamma} p|_{x_2=0}\,\mathrm{d}x_1 = Ra\int_{\Omega} T\,\partial_2 p\,\mathrm{d}x$ thanks to the boundary conditions for T.

Argument for (2.50). Since $\boldsymbol{u}$ is divergence-free, we have

$$0 = \int_{\Omega} p(-1 + 2x_2)\,\partial_2(\nabla \cdot \boldsymbol{u})\,\mathrm{d}x = \int_{\Omega} p(-1 + 2x_2)\,\nabla \cdot (\partial_2 \boldsymbol{u})\,\mathrm{d}x, \tag{2.57}$$

and integration by parts yields

$$\int_{\Omega} p(-1+2x_2)\,\nabla\cdot(\partial_2 \boldsymbol{u})\,\mathrm{d}x = -\int_{\Omega} \nabla p\cdot(-1+2x_2)\,\partial_2\boldsymbol{u}\,\mathrm{d}x - 2\int_{\Omega} p\,\partial_2 u_2\,\mathrm{d}x$$
$$-\left(\int_0^{\Gamma} p\,\partial_1 u_1|_{x_2=1} + p\,\partial_1 u_1|_{x_2=0}\right)\mathrm{d}x_1, \tag{2.58}$$

where we used $\partial_1 u_1 = -\partial_2 u_2$ by incompressibility. Combining the two identities, we obtain

$$\left|\int_0^{\Gamma} (p\,\partial_1 u_1|_{x_2=1} + p\,\partial_1 u_1|_{x_2=0})\,\mathrm{d}x_1\right| \leq 2\,\|p\|_{L^2}\,\|\partial_2 u_2\|_{L^2} + \|\partial_2\boldsymbol{u}\|_{L^2}\,\|\nabla p\|_{L^2} \tag{2.59}$$
$$\leq 3\,\|p\|_{H^1}\,\|\partial_2\boldsymbol{u}\|_{L^2}. \tag{2.60}$$

REMARK 2.6. *The pressure bound in Proposition 2.7 of Drivas et al. (2022) is given by*

$$\|p\|_{H^1} \leq C\left(\frac{1}{L_s}\,\|\partial_1\omega\|_{L^2} + \frac{1}{Pr}\,\|\omega\|_{L^2}\,\|\omega\|_{L^r} + Ra\,\|T\|_{L^2}\right). \tag{2.61}$$

In the subsequent analysis, the authors bound the term $(1/L_s)\,\|\partial_1\omega\|_{L^2}$ from above with $\|\nabla\omega\|_{L^2}$, imposing the condition that $L_s \geq 1$. In contrast, using the refined estimate (2.48), we are able to treat any slip length $L_s > 0$, improving the scaling of Nu with respect to Ra.

We conclude this section with bounds on second derivatives of the velocity field. First, we relate the L^2-norm of $\nabla^2\boldsymbol{u}$ to the L^2-norm of $\nabla\omega$.

LEMMA 2.7.

$$\|\nabla^2\boldsymbol{u}\|_{L^2} \leq \|\nabla\omega\|_{L^2}. \tag{2.62}$$

Proof. First, we show that $\|\nabla^2\boldsymbol{u}\|_{L^2} \leq \|\Delta\boldsymbol{u}\|_{L^2}$: integrating by parts twice yields

$$\|\nabla^2\boldsymbol{u}\|^2_{L^2(\Omega)} = \int_{\Omega} \partial_i\partial_j u_k\,\partial_i\partial_j u_k\,\mathrm{d}x \tag{2.63}$$
$$= \int_{\Omega} \partial_i^2 u_k\,\partial_j^2 u_k\,\mathrm{d}x - \int_{\partial\Omega} \partial_i^2 u_k\,\partial_j u_k n_j\,\mathrm{d}S + \int_{\partial\Omega} \partial_i\partial_j u_k\,\partial_j u_k n_i\,\mathrm{d}S \tag{2.64}$$
$$= \|\Delta\boldsymbol{u}\|^2_{L^2(\Omega)} - \int_0^{\Gamma} \partial_1^2 u_k\,\partial_2 u_k n_2\,\mathrm{d}x_1 + \int_0^{\Gamma} \partial_2\partial_1 u_k\,\partial_1 u_k n_2\,\mathrm{d}x_1, \tag{2.65}$$

where we used periodicity in the horizontal direction and the fact that the terms with $i=j$ cancel. Note that due to (1.9), the boundary terms have a sign:

$$-\int_0^{\Gamma} \partial_1^2 u_k\,\partial_2 u_k n_2\,\mathrm{d}x_1 + \int_0^{\Gamma} \partial_2\partial_1 u_k\,\partial_1 u_k n_2\,\mathrm{d}x_1$$
$$= -\int_0^{\Gamma} \partial_1^2 u_1\,\partial_2 u_1 n_2\,\mathrm{d}x_1 + \int_0^{\Gamma} \partial_2\partial_1 u_1\,\partial_1 u_1 n_2\,\mathrm{d}x_1 \tag{2.66}$$
$$= \frac{1}{L_s}\int_0^{\Gamma} \partial_1^2 u_1 u_1\,\mathrm{d}x_1 - \int_0^{\Gamma} (\partial_1 u_1)^2\,\mathrm{d}x_1 = -\frac{2}{L_s}\int_0^{\Gamma} (\partial_1 u_1)^2\,\mathrm{d}x_1 \leq 0, \tag{2.67}$$

where in the last identity we used the periodicity in the horizontal direction. This proves the first claim.

Now, a direct computation yields $\Delta \boldsymbol{u} = \nabla^{\perp}\omega$, and from this follows $\|\Delta \boldsymbol{u}\|_{L^2(\Omega)} = \|\nabla\omega\|_{L^2(\Omega)}$. We conclude that

$$\|\nabla^2 \boldsymbol{u}\|_{L^2(\Omega)} \leq \|\Delta \boldsymbol{u}\|_{L^2(\Omega)} = \|\nabla\omega\|_{L^2(\Omega)}, \tag{2.68}$$

yielding (2.62).

Next, we relate $\|\nabla^2 \boldsymbol{u}\|_{L^2}$ to Nu, Ra and L_s, via an upper bound for $\|\nabla\omega\|_{L^2}$. This is done by combining (2.42), the pressure bound (2.48) and the boundary integral estimate (2.50). The resulting bound on the long-time average of the velocity Hessian together with the corresponding bound on the velocity gradient of Lemma 2.10 are key ingredients in order to estimate the boundary layer thickness in the proof of the main theorem.

LEMMA 2.8 (Hessian bound). *Let $L_s > 0$ and $\boldsymbol{u}_0 \in W^{1,4}$. Then there exists a constant $C = C(\Gamma) > 0$ such that*

$$\left\langle \|\nabla^2 \boldsymbol{u}\|_{L^2}^2 \right\rangle \leq C \left(L_s^{-2} + \frac{\max\{1, L_s^{-3}\}\,(\|\boldsymbol{u}_0\|_{W^{1,4}} + Ra)}{Pr\, L_s} + L_s^{-1}\, Nu^{-1/2}\, Ra^{1/2} + Ra^{1/2} \right) Nu\, Ra. \tag{2.69}$$

Proof. From (2.62) and (2.42), we have

$$\left\langle \int_0^1 |\nabla^2 \boldsymbol{u}|^2 \,\mathrm{d}x \right\rangle \leq L_s^{-1} \left(\langle p\, \partial_1 u_1|_{x_2=1} \rangle + \langle p\, \partial_1 u_1|_{x_2=0} \rangle \right) + Nu\, Ra^{3/2}. \tag{2.70}$$

Using (2.50) and (2.48), we obtain

$$\left\langle \int_0^1 |\nabla^2 \boldsymbol{u}|^2 \,\mathrm{d}x \right\rangle \leq L_s^{-1} \langle \|p\|_{H^1} \|\partial_2 \boldsymbol{u}\|_{L^2} \rangle + Nu\, Ra^{3/2} \tag{2.71}$$

$$\leq L_s^{-2} \langle \|\partial_2 \boldsymbol{u}\|_{L^2}^2 \rangle + L_s^{-1}\, Pr^{-1} \langle \|\omega\|_{L^2}\, \|\omega\|_{L^4}\, \|\partial_2 \boldsymbol{u}\|_{L^2} \rangle + L_s^{-1}\, Ra\, \langle \|T\|_{L^2}\, \|\partial_2 \boldsymbol{u}\|_{L^2} \rangle + Nu\, Ra^{3/2}. \tag{2.72}$$

For the L^4-norm of the vorticity, the pointwise (in time) bound (2.41) states

$$\|\omega(t)\|_{L^4} \leq C \max\left\{1, L_s^{-3}\right\} (\|\boldsymbol{u}_0\|_{W^{1,4}} + Ra), \tag{2.73}$$

for some constant $C > 0$ depending only on Γ. Therefore, additionally using the identity (2.32), (2.72) can be estimated as follows:

$$\left\langle \int_0^1 |\nabla^2 \boldsymbol{u}|^2 \,\mathrm{d}x_2 \right\rangle \leq L_s^{-2} \langle \|\partial_2 \boldsymbol{u}\|_{L^2}^2 \rangle + \frac{C \max\{1, L_s^{-3}\}}{Pr\, L_s} \langle \|\nabla \boldsymbol{u}\|_{L^2} (\|\boldsymbol{u}_0\|_{W^{1,4}} + Ra)\, \|\partial_2 \boldsymbol{u}\|_{L^2} \rangle + L_s^{-1}\, Ra\, \langle \|T\|_{L^2}\, \|\partial_2 \boldsymbol{u}\|_{L^2} \rangle + Nu\, Ra^{3/2}. \tag{2.74}$$

Finally, using $\langle \|\partial_2 \boldsymbol{u}\|_{L^2}^2 \rangle \leq \langle \|\nabla \boldsymbol{u}\|_{L^2}^2 \rangle$, the upper bound in (2.10) and the maximum principle for the temperature (2.1), we deduce

$$\left\langle \int_0^1 |\nabla^2 \boldsymbol{u}|^2 \,\mathrm{d}x_2 \right\rangle \leq L_s^{-2}\, Nu\, Ra + \frac{C \max\{1, L_s^{-3}\}}{Pr\, L_s} (\|\boldsymbol{u}_0\|_{W^{1,4}} + Ra)\, Nu\, Ra + L_s^{-1}\, \Gamma^{1/2}\, Nu^{1/2}\, Ra^{3/2} + Nu\, Ra^{3/2}. \tag{2.75}$$

3. Proof of Theorem 1.1

A crucial ingredient of the proof of Theorem 1.1 is the following interpolation bound, relating the integral of the product u_2T with $\|\nabla T\|_{L^2}$, $\|\nabla \boldsymbol{u}\|_{L^2}$ and $\|\nabla^2 \boldsymbol{u}\|_{L^2}$. Notice that, in turn, these quantities are estimated in terms of Nusselt, Rayleigh and Prandtl numbers in (2.7), (2.10) and (2.69).

LEMMA 3.1. *The interpolation bound*

$$\frac{1}{\delta}\left\langle \int_0^\delta u_2 T \,\mathrm{d}x_2 \right\rangle \le \frac{1}{2}\left\langle \int_0^1 |\partial_2 T|^2 \,\mathrm{d}x_2 \right\rangle + C\delta^3 \left\langle \int_0^1 |\nabla \boldsymbol{u}|^2 \,\mathrm{d}x_2 \right\rangle^{1/2} \left\langle \int_0^1 |\nabla^2 \boldsymbol{u}|^2 \,\mathrm{d}x_2 \right\rangle^{1/2} \tag{3.1}$$

holds for some constant $C > 0$.

Proof. First, notice that due to incompressibility $\partial_2 u_2 = -\partial_1 u_1$ and horizontal periodicity,

$$\partial_2 \frac{1}{\Gamma}\int_0^\Gamma u_2(x_1, x_2)\,\mathrm{d}x_1 = -\frac{1}{\Gamma}\int_0^\Gamma \partial_1 u_1(x_1, x_2)\,\mathrm{d}x_1 = 0, \tag{3.2}$$

implying

$$\frac{1}{\Gamma}\int_0^\Gamma u_2(x_1, x_2)\,\mathrm{d}x_1 = 0 \tag{3.3}$$

thanks to the boundary conditions $u_2 = 0$ at $x_2 = \{0, 1\}$. Let $\theta(x_1, x_2) := T(x_1, x_2) - 1$; then $\theta(x_1, x_2) = 0$ at $x_2 = 0$, and by (3.3),

$$\frac{1}{\delta}\left\langle \int_0^\delta u_2 T \,\mathrm{d}x_2 \right\rangle = \frac{1}{\delta}\left\langle \int_0^\delta u_2 \theta \,\mathrm{d}x_2 \right\rangle. \tag{3.4}$$

By the fundamental theorem of calculus and the homogeneous Dirichlet boundary conditions for θ and u_2, we have

$$|\theta(x_1, x_2)| \le x_2^{1/2}\, \|\partial_2\theta\|_{L^2(0,1)}, \tag{3.5}$$

$$|u_2(x_1, x_2)| \le x_2\, \|\partial_2 u_2\|_{L^\infty(0,1)}. \tag{3.6}$$

Furthermore, since $\int_0^1 \partial_2 u_2(x_1, x_2)\,\mathrm{d}x_2 = 0$, there exists $\xi = \xi(x_1) \in (0, 1)$ such that $\partial_2 u_2(x_1, \xi) = 0$. Then

$$|\partial_2 u_2(x_1, x_2)|^2 = \left| \int_\xi^{x_2} \partial_2(\partial_2 u_2(x_1, z))^2 \,\mathrm{d}z \right| = \left| 2\int_\xi^{x_2} \partial_2 u_2\, \partial_2^2 u_2 \,\mathrm{d}z \right|, \tag{3.7}$$

which implies

$$|u_2(x_1, x_2)| \le x_2\, \|\partial_2 u_2(x_1, \cdot)\|_{L^2(0,1)}^{1/2}\, \|\partial_2^2 u_2(x_1, \cdot)\|_{L^2(0,1)}^{1/2}. \tag{3.8}$$

Combining these estimates, we obtain

$$\frac{1}{\delta}\left\langle \int_0^\delta u_2\theta \, \mathrm{d}x_2 \right\rangle$$

$$\leq \frac{1}{\delta}\left\langle \int_0^\delta x_2^{3/2} \, \|\partial_2 u_2(x_1,\cdot)\|_{L^2(0,1)} \, \|\partial_2^2 u_2(x_1,\cdot)\|_{L^2(0,1)} \, \|\partial_2\theta(x_1,\cdot)\|^2_{L^2(0,1)} \, \mathrm{d}x_2 \right\rangle \quad (3.9)$$

$$\leq \delta^{3/2}\left\langle \|\partial_2 u_2(x_1,\cdot)\|_{L^2(0,1)} \, \|\partial_2^2 u_2(x_1,\cdot)\|_{L^2(0,1)} \right\rangle^{1/2} \left\langle \|\partial_2\theta(x_1,\cdot)\|^2_{L^2(0,1)} \right\rangle^{1/2} \quad (3.10)$$

$$\leq C\delta^3\left\langle \|\partial_2 u_2(x_1,\cdot)\|^2_{L^2(0,1)} \right\rangle^{1/2} \left\langle \|\partial_2^2 u_2(x_1,\cdot)\|^2_{L^2(0,1)} \right\rangle^{1/2} + \frac{1}{2}\left\langle \|\partial_2\theta(x_1,\cdot)\|^2_{L^2(0,1)} \right\rangle. \quad (3.11)$$

3.1. *Case $L_s = \infty$*

In this subsection, we prove the upper bound (1.17) when $L_s = \infty$ in (1.9), re-deriving the seminal result of Whitehead & Doering (2011) with a different technique. While the proof in Whitehead & Doering (2011) is a sophisticated application of the background field method, our new proof for the $Ra^{5/12}$ scaling is a pure partial differential equation argument based on the combination of the localization principle together with the interpolation bound (1.22).

We first notice that setting $L_s = \infty$ in (2.10), (2.32) and (2.42), we obtain

$$\left\langle \int_0^1 |\omega|^2 \, \mathrm{d}x_2 \right\rangle = \left\langle \int_0^1 |\nabla \boldsymbol{u}|^2 \, \mathrm{d}x_2 \right\rangle \leq Nu\, Ra, \quad (3.12)$$

$$\left\langle \int_0^1 |\partial_1\omega|^2 \, \mathrm{d}x_2 \right\rangle \leq \left\langle \int_0^1 |\nabla \omega|^2 \, \mathrm{d}x_2 \right\rangle \leq Nu\, Ra^{3/2}. \quad (3.13)$$

Combining these upper bounds and the identity (2.7) in the localization estimate (1.21), we find

$$Nu \leq \frac{1}{2} Nu + C\delta^3 (Nu\, Ra)^{1/2} (Ra^{3/2}\, Nu)^{1/2} + \frac{1}{\delta}, \quad (3.14)$$

which yields

$$\frac{1}{2} Nu \leq C\delta^3\, Nu\, Ra^{5/4} + \frac{1}{\delta}. \quad (3.15)$$

Optimizing in δ,

$$\delta \sim \frac{1}{Ra^{5/16}\, Nu^{1/4}}, \quad (3.16)$$

we deduce

$$Nu \lesssim Ra^{5/12}. \quad (3.17)$$

3.2. *Case* $0 < L_s < \infty$

Using the localization of the Nusselt number (2.6) and (3.1), we have

$$Nu \leq \frac{1}{\delta}\left\langle \int_0^\delta u_2 T \, \mathrm{d}x_2 \right\rangle + \frac{1}{\delta} \tag{3.18}$$

$$\leq \frac{1}{2}\left\langle \int_0^1 |\nabla T|^2 \, \mathrm{d}x_2 \right\rangle + C\delta^3 \left\langle \int_0^1 |\nabla \boldsymbol{u}|^2 \, \mathrm{d}x_2 \right\rangle^{1/2} \left\langle \int_0^1 |\nabla^2 \boldsymbol{u}|^2 \, \mathrm{d}x_2 \right\rangle^{1/2} + \frac{1}{\delta}, \tag{3.19}$$

yielding

$$\frac{1}{2} Nu \leq C\delta^3 \left\langle \int_0^\delta |\nabla \boldsymbol{u}|^2 \, \mathrm{d}x_2 \right\rangle^{1/2} \left\langle \int_0^1 |\nabla^2 \boldsymbol{u}|^2 \, \mathrm{d}x_2 \right\rangle^{1/2} + \frac{1}{\delta}, \tag{3.20}$$

where we used (2.7). Finally, we insert the bounds (2.10) and (2.69) in the last inequality, and if Ra is large enough such that $\|\boldsymbol{u}_0\|_{W^{1,4}} \lesssim Ra$, then up to redefining constants, we find

$$Nu \leq C\delta^3 \left(L_s^{-1} \, Nu \, Ra + \max\{1, L_s^{-3/2}\} \, L_s^{-1/2} \, Pr^{-1/2} \, Nu \, Ra^{3/2} + L_s^{-1/2} \, Nu^{3/4} \, Ra^{5/4} + Nu \, Ra^{5/4} \right) + \frac{2}{\delta}. \tag{3.21}$$

We first cover the case $L_s \geq 1$. Then, as $L_s, Nu \geq 1$, the first and third terms on the right-hand side of (3.21) are dominated by $Nu \, Ra^{5/4}$, hence

$$Nu \leq C\delta^3 \, Nu \left(L_s^{-1/2} \, Pr^{-1/2} \, Ra^{3/2} + Ra^{5/4} \right) + 2\delta^{-1}, \tag{3.22}$$

and optimizing by setting $\delta = Nu^{-1/4} (L_s^{-1/2} \, Pr^{-1/2} \, Ra^{3/2} + Ra^{5/4})^{-1/4}$ implies

$$Nu \lesssim L_s^{-1/6} \, Pr^{-1/6} \, Ra^{1/2} + Ra^{5/12}. \tag{3.23}$$

If instead $L_s < 1$, then (3.21) is given by

$$Nu \leq C\delta^3 \left(L_s^{-1} \, Nu \, Ra + L_s^{-2} \, Pr^{-1/2} \, Nu \, Ra^{3/2} + L_s^{-1/2} \, Nu^{3/4} \, Ra^{5/4} + Nu \, Ra^{5/4} \right) + 2\delta^{-1}. \tag{3.24}$$

Optimizing by setting

$$\delta = \begin{cases} Nu^{-1/4} \left(L_s^{-1} \, Ra + L_s^{-2} \, Pr^{-1/2} \, Ra^{3/2} + Ra^{5/4} \right)^{-1/4}, & \text{if } L_s^{-1/2} \, Ra^{-1/4} + L_s^{-3/2} \, Pr^{-1/2} \, Ra^{1/4} + L_s^{1/2} \geq Nu^{-1/4}, \\ L_s^{1/8} \, Nu^{-3/16} \, Ra^{-5/16}, & \text{if } L_s^{-1/2} \, Ra^{-1/4} + L_s^{-3/2} \, Pr^{-1/2} \, Ra^{1/4} + L_s^{1/2} \leq Nu^{-1/4}, \end{cases} \tag{3.25}$$

yields

$$Nu \lesssim L_s^{-1/3} \, Ra^{1/3} + L_s^{-2/3} \, Pr^{-1/6} \, Ra^{1/2} + L_s^{-2/13} \, Ra^{5/13} + Ra^{5/12}. \tag{3.26}$$

4. Conclusion

Our work is motivated by recent investigations in Whitehead & Doering (2011) and Drivas *et al.* (2022) indicating that variations in the boundary conditions for the velocity affect heat transport properties in Rayleigh–Bénard convection. The Navier-slip boundary conditions are prescribed in the situation in which some slip occurs on the surface, and at the same time stress is exerted on the fluid. In particular, the use of these boundary conditions is justified when the scale of interest goes down to microns or below, when the no-slip boundary conditions cease to be valid (see Choi & Kim 2006). Mathematically, these boundary conditions are referred to as 'interpolation' boundary conditions since they represent a situation in between the physically relevant, but very difficult to treat, no-slip boundary conditions and the easier, but unphysical, free-slip boundary conditions. When free-slip boundary conditions are considered, the key tool in order to control the growth of the vertical velocity u_2 near the boundaries is the enstrophy balance (Whitehead & Doering 2011, 2012; Wang & Whitehead 2013). When Navier-slip boundary conditions are considered instead, the control of enstrophy production becomes difficult since the pressure term and the vertical derivative of u_2, $\partial_2 u_2 = -\partial_1 u_1$, appear at the boundary; see (2.42). This problem was already tackled in Drivas *et al.* (2022), and in this paper, we improve this control by refining the trace estimates; see (2.50). In Bleitner & Nobili (2024), the analysis in Drivas *et al.* (2022) was extended to rough boundary conditions, capturing the dependency of the scaling from the spatially varying friction coefficient and curvature. To our knowledge, no other rigorous results are available for the Nusselt number in this set-up.

In the same setting as considered in the present paper, direct numerical simulations (DNS) were performed in Huang & He (2022) to study the scaling of the Nusselt number in the convective roll state and in the zonal flow (turbulent state). The authors found that, when $L_s/\lambda_0 \lesssim 10$ (here the slip length is normalized by λ_0, the thermal boundary layer thickness for the no-slip plates), $Nu \sim Ra^{0.31}$ in the convection roll state. In particular, they observe that in the convection roll state, for a fixed Ra, the heat transfer Nu increases with increasing L_s/λ_0. On the other hand, they observe that in the zonal flow, the heat transport Nu decreases with increasing L_s/λ_0 at fixed Ra. They explain this phenomenon as being due to the reduction of the vertical Reynolds number: as L_s/λ_0 increases, the zonal flow becomes stronger, and it suppresses the vertical velocity, leading to a decrease in Nu. In this regime, their DNS indicate the scaling $Nu \sim Ra^{0.16}$. As can be noticed in table 1, our rigorous upper bounds indicate a behaviour in agreement with the results in Huang & He (2022): in the turbulent regime, as the slip length L_s increases, the heat transport decreases. In fact, observe that in each Pr region, the heat transport increases from $Nu \lesssim Ra^{5/12}$ when $L_s = \infty$, to $Nu \lesssim L_s^{-2/3}\, Pr^{-1/6}\, Ra^{1/2}$ when $L_s < 1$ (see table 1, where the upper bounds are ordered from the smallest to the largest in each Pr region). Let us recall that for no-slip boundary conditions ($L_s = 0$) Otto, Choffrut and the second author of this paper find $Nu \lesssim (Ra\ln(Ra))^{1/3}$ when $Pr \gtrsim (Ra\ln(Ra))^{1/3}$ and $Nu \lesssim Pr^{-1/2}(Ra\ln(Ra))^{1/2}$ when $Pr \lesssim (Ra\ln(Ra))^{1/3}$ (Choffrut *et al.* 2016), while Doering & Constantin (1996) prove $Nu \lesssim Ra^{1/2}$ uniformly in Pr. In the regime of small L_s, our upper bound is $Nu \lesssim L_s^{-2/3}\, Pr^{-1/6}\, Ra^{1/2}$ for any Prandtl number. We cannot directly compare the results in the present paper with the results available for no-slip boundary conditions in Choffrut *et al.* (2016) and Doering & Constantin (1996) since our analysis breaks down in the limit $L_s \to 0$. With respect to the long-standing open problem regarding the scaling laws for the Nusselt number in the 'ultimate state' (Zhu

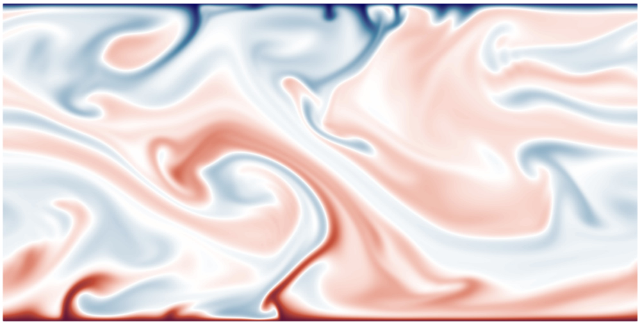

Figure 1. Thermal boundary layers arising at $Pr = 1$, $L_s = 1$ and $Ra = 10^8$. This snapshot is generated by a simulation.

et al. 2018, 2019; Doering *et al.* 2019; Doering 2020), we can say the following. On the one hand, the DNS in Huang & He (2022) and our analysis seem to suggest that, for any Prandtl number region and any $L_s \neq 0$, the Malkus scaling $Nu \sim Ra^{1/3}$ is not achievable in the turbulent regime. This is quite evident when looking at the results in table 1, since (as mentioned before) the upper bounds are ordered and increase from $Ra^{5/12}$ as L_s decreases. However, we warn that the reality of heat transport might be much more complicated than this nice picture. With our arguments we are able to derive only upper bounds, and cannot exclude the possibility of smaller scaling exponents. Indeed, one of the biggest theoretical challenges for this problem is to find (non-trivial) lower bounds for the Nusselt number. Even just exhibiting solutions that attain certain upper bounds in some simplified situation (in the spirit of Souza & Doering 2015) would be a big step ahead in the theory. Interesting ideas in this direction have been developed by Tobasco & Doering (2017) and Tobasco (2022): inspired by problems arising in the study of energy-driven pattern formation in materials science, the authors design a two-dimensional 'branching' flow that transports at rate $Nu \sim Pe^{2/3}$ (up to a logarithmic correction) for a passive tracer that diffuses and is advected by a divergence-free velocity field with a fixed enstrophy budget $\langle \|\nabla \boldsymbol{u}\|_{L^2}^2 \rangle \sim Pe^2$. Here, Pe is the Péclet number. The remarkable lower bound that they derive using 'branching' techniques is responsible for the logarithmic corrections. Although their result in particular shows that the $Ra^{1/2}$ 'ultimate' scaling is attained by flows that do not solve (1.1)–(1.3), these arguments can be used to detect mechanisms that make the scalings $Ra^{1/2}$ and $Ra^{1/3}$ realizable for buoyancy-driven solutions.

Finally, we want to conclude with a remark. Our upper bounds on the Nusselt number quantify heat transport properties of the (thermal) boundary layer without characterizing it. The only information that we can extrapolate from our analysis is about the (thermal) boundary layer thickness (see figure 1). On the other hand, in the excellent work Gie & Whitehead (2019), the authors are able to describe the flow in the boundary layer. In a three-dimensional periodic channel, they study the Boussinesq system at very small viscosities and with Navier-slip boundary conditions. Through the explicit construction of a corrector, they show that the behaviour of the dynamics in the boundary layers is governed by the Prandtl equations. In particular, these equations can be linearized for Navier-slip boundary conditions, implying that in this specific case, the boundary layers are non-turbulent. From this, the authors deduce that the 'ultimate' state, which is based on the hypothesis of a turbulent boundary layer (Ahlers, Grossmann & Lohse 2009), cannot exist in this particular set-up.

Acknowledgements. The authors acknowledge support by the Deutsche Forschungsgemeinschaft (DFG) within the Research Training Group GRK 2583 'Modeling, Simulation and Optimization of Fluid Dynamic Applications.'

Declaration of interests. The authors report no conflict of interest.

Author ORCIDs.
F. Bleitner https://orcid.org/0000-0001-9865-7163;
C. Nobili https://orcid.org/0000-0001-6976-7494.

REFERENCES

AHLERS, G. 2006 Experiments with Rayleigh–Bénard convection. In *Dynamics of Spatio-Temporal Cellular Structures: Henri Bénard Centenary Review* (ed. I. Mutabazi, J.E. Wesfreid & E. Guyon), pp. 67–94. Springer.

AHLERS, G., GROSSMANN, S. & LOHSE, D. 2009 Heat transfer and large scale dynamics in turbulent Rayleigh–Bénard convection. *Rev. Mod. Phys.* **81** (2), 503–537.

BLEITNER, F. & NOBILI, C. 2024 Bounds on buoyancy driven flows with Navier-slip conditions on rough boundaries. *Nonlinearity* **37** (3), 035017.

CHERNYSHENKO, S. 2022 Relationship between the methods of bounding time averages. *Phil. Trans. R. Soc.* A **380** (2225), 20210044.

CHOFFRUT, A., NOBILI, C. & OTTO, F. 2016 Upper bounds on Nusselt number at finite Prandtl number. *J. Differ. Equ.* **260** (4), 3860–3880.

CHOI, C.-H. & KIM, C.-J. 2006 Large slip of aqueous liquid flow over a nanoengineered superhydrophobic surface. *Phys. Rev. Lett.* **96** (6), 066001.

DOERING, C.R. 2020 Absence of evidence for the ultimate state of turbulent Rayleigh–Bénard convection. *Phys. Rev. Lett.* **124** (22), 229401.

DOERING, C.R. & CONSTANTIN, P. 1994 Variational bounds on energy dissipation in incompressible flows: shear flow. *Phys. Rev.* E **49** (5), 4087–4099.

DOERING, C.R. & CONSTANTIN, P. 1996 Variational bounds on energy dissipation in incompressible flows. III. Convection. *Phys. Rev.* E **53** (6), 5957–5981.

DOERING, C.R. & CONSTANTIN, P. 2001 On upper bounds for infinite Prandtl number convection with or without rotation. *J. Math. Phys.* **42** (2), 784–795.

DOERING, C.R., OTTO, F. & REZNIKOFF, M.G. 2006 Bounds on vertical heat transport for infinite-Prandtl-number Rayleigh–Bénard convection. *J. Fluid Mech.* **560**, 229–241.

DOERING, C.R., TOPPALADODDI, S. & WETTLAUFER, J.S. 2019 Absence of evidence for the ultimate regime in two-dimensional Rayleigh–Bénard convection. *Phys. Rev. Lett.* **123** (25), 259401.

DRIVAS, T.D., NGUYEN, H.Q. & NOBILI, C. 2022 Bounds on heat flux for Rayleigh–Bénard convection between Navier-slip fixed-temperature boundaries. *Phil. Trans. R. Soc.* A **380** (2225), 20210025.

EVANS, L.C. 1998 *Partial Differential Equations*, 2nd edn, vol. 19. Graduate Studies in Mathematics. American Mathematical Society.

GIE, G.-M. & WHITEHEAD, J.P. 2019 Boundary layer analysis for Navier-slip Rayleigh–Bénard convection: the non-existence of an ultimate state. *J. Math. Fluid Mech.* **21**, 1–25.

GILBARG, D. & TRUDINGER, N.S. 1977 *Elliptic Partial Differential Equations of Second Order*, vol. 224. Grundlehren der mathematischen Wissenschaften. Springer.

GOLUSKIN, D. & DOERING, C.R. 2016 Bounds for convection between rough boundaries. *J. Fluid Mech.* **804**, 370–386.

HUANG, M. & HE, X. 2022 Effect of slip length on flow dynamics and heat transport in two-dimensional Rayleigh–Bénard convection. *J. Turbul.* **23** (9–10), 492–514.

IERLEY, G.R., KERSWELL, R.R. & PLASTING, S.C. 2006 Infinite-Prandtl-number convection. Part 2. A singular limit of upper bound theory. *J. Fluid Mech.* **560**, 159–227.

KRAICHNAN, R.H. 1962 Turbulent thermal convection at arbitrary Prandtl number. *Phys. Fluids* **5** (11), 1374–1389.

MALKUS, W.V.R. 1954 The heat transport and spectrum of thermal turbulence. *Proc. R. Soc. Lond.* A **225** (1161), 196–212.

NETO, C., EVANS, D.R., BONACCURSO, E., BUTT, H.-J. & CRAIG, V.S.J. 2005 Boundary slip in Newtonian liquids: a review of experimental studies. *Rep. Prog. Phys.* **68** (12), 2859.

NOBILI, C. 2023 The role of boundary conditions in scaling laws for turbulent heat transport. *Maths Engng* **5** (1), 1–41.

OTERO, J. 2002 *Bounds for the Heat Transport in Turbulent Convection*. University of Michigan.
OTTO, F. & SEIS, C. 2011 Rayleigh–Bénard convection: improved bounds on the Nusselt number. *J. Math. Phys.* **52** (8), 083702.
PLUMLEY, M. & JULIEN, K. 2019 Scaling laws in Rayleigh–Bénard convection. *Earth Space Sci.* **6** (9), 1580–1592.
SIGGIA, E.D. 1994 High Rayleigh number convection. *Annu. Rev. Fluid Mech.* **26** (1), 137–168.
SOUZA, A.N. & DOERING, C.R. 2015 Maximal transport in the Lorenz equations. *Phys. Lett.* A **379** (6), 518–523.
SPIEGEL, E.A. 1971 Convection in stars I. Basic Boussinesq convection. *Annu. Rev. Astron. Astrophys.* **9** (1), 323–352.
TOBASCO, I. 2022 Optimal cooling of an internally heated disc. *Phil. Trans. R. Soc.* A **380** (2225), 20210040.
TOBASCO, I. & DOERING, C.R. 2017 Optimal wall-to-wall transport by incompressible flows. *Phys. Rev. Lett.* **118** (26), 264502.
UTHE, B., SADER, J.E. & PELTON, M. 2022 Optical measurement of the picosecond fluid mechanics in simple liquids generated by vibrating nanoparticles: a review. *Rep. Prog. Phys.* **85** (10), 103001.
WANG, X. & WHITEHEAD, J.P. 2013 A bound on the vertical transport of heat in the 'ultimate' state of slippery convection at large Prandtl numbers. *J. Fluid Mech.* **729**, 103–122.
WHITEHEAD, J.P. & DOERING, C.R. 2011 Ultimate state of two-dimensional Rayleigh–Bénard convection between free-slip fixed-temperature boundaries. *Phys. Rev. Lett.* **106**, 244501.
WHITEHEAD, J.P. & DOERING, C.R. 2012 Rigid bounds on heat transport by a fluid between slippery boundaries. *J. Fluid Mech.* **707**, 241–259.
ZHU, X., MATHAI, V., STEVENS, R.J.A.M., VERZICCO, R. & LOHSE, D. 2018 Transition to the ultimate regime in two-dimensional Rayleigh–Bénard convection. *Phys. Rev. Lett.* **120** (14), 144502.
ZHU, X., MATHAI, V., STEVENS, R.J.A.M., VERZICCO, R. & LOHSE, D. 2019 Zhu *et al.* reply. *Phys. Rev. Lett.* **123** (25), 259402.